Paste 2026 – AB Fourie, M Horta, M Oliveira & S Wilson (eds)

doi:10.36487/ACG_repo/2655_39

Applying the material point method for *Global Industry Standard on Tailings Management* compliance

Alejandro Kerguelen [a,*], Alejandro Calvo [a], Mateo Sepúlveda [a], Diego Cobos [a], Arcesio Lizcano [b]

[a] *SRK Consulting, Colombia*

[b] *SRK Consulting, Canada*

Abstract

The Global Industry Standard on Tailings Management *(GISTM) requires credible failure–scenario assessments and consequence zoning. Current practice, guided by the Canadian Dam Association (2021), prioritises water-laden tailings with hydraulic entrainment (Cases 1A and 1B) leaving solids-dominated releases (Cases 2A and 2B) less explored. This work extends routine assessment to such cases using the material point method (MPM) – a large-deformation numerical technique suited to solid-dominated failures where interparticle friction and shear strength control post-failure and runout.*

The methodology is illustrated through 3 case studies: a conventional tailings storage facility (TSF) with a pond located at the toe of the dam, a compacted filtered TSF placed over a waste rock dump, and a compacted filtered TSF located in a valley. The results provide estimated runout distances under these conditions, highlighting MPM's capability to support GISTM compliance and comprehensive risk evaluations.

Keywords: Global Industry Standard on Tailings Management*, material point method, solids-dominated failure, compacted filtered tailings, runout*

1 Introduction

Tailings dam breach analysis has become a critical component of risk-informed design and governance under the *Global Industry Standard on Tailings Management* (GISTM). The standard requires operators and engineers of record to identify credible failure scenarios and quantify downstream impacts through defensible dam breach and runout analyses. To support this process, the Canadian Dam Association (CDA) (CDA 2021) provides a structured framework for defining representative tailings release scenarios based primarily on water availability and liquefaction potential. This framework distinguishes between water-dominated releases (Cases 1A and 1B) and solids-dominated releases (Cases 2A and 2B), each governed by fundamentally different post-failure mechanics (Figure 1).

Historical failures demonstrate the strong influence of water content and deposition state on both the failure mechanism and the resulting mobility of released materials. Conventional slurry impoundment failures such as Fundão (Brazil 2015) and Brumadinho (Brazil 2019) involved breach development followed by extensive hydraulic entrainment and long-distance mudflow behaviour consistent with fluidised tailings releases (Morgenstern et al. 2016; Robertson et al. 2019). In contrast, failures involving paste, filtered, or otherwise dewatered deposits frequently manifest primarily as geomechanical slope instabilities rather than classical hydraulic breaches. For example, the incident at the Las Cenizas mining operation in Cabildo, Chile, in 2024 involved collapse of paste tailings containment during intense rainfall, producing release through mass sliding rather than rapid hydraulic erosion (BioBioChile 2024; Reporte Minero 2025). Similarly, in the same year, the slope failure at the Turmalina Mine in Brazil involved large-scale slumping of dry-stack tailings and waste rock pile, consistent with landslide-type movement (Jaguar Mining Inc 2024; Petley 2024).

* Corresponding author. Email address: akerguelen@srk.co

These recent solids-dominated failures demonstrate that non-conventional facilities with limited free water – such as compacted filtered tailings stacks, co-disposal systems, and paste deposits – are governed by additional mechanisms, including progressive shear strength degradation, block-type sliding, and granular collapse. In these cases, post-failure mobility is controlled primarily by soil mechanics rather than by fluid dynamics. Despite this, current engineering practice continues to rely predominantly on breach modelling methodologies and software tools formulated within hydrodynamic routing or simplified rheological frameworks, which may not adequately represent strength-controlled deformation processes in largely dewatered tailings systems. Consequently, the released material is often assumed to behave as a fluid even in dewatered tailings facilities or when mechanically stable. This simplification may lead to unrealistic runout distances and inflated inundation footprints, which directly influence consequence classification and risk management decisions under the GISTM framework.

To address this limitation, this study adopts the material point method (MPM) – a large-deformation numerical technique increasingly used in geotechnical research and practice to simulate the post-failure response of tailings under strength-controlled conditions. The approach is illustrated through 3 case studies:

1. A conventional tailings storage facility (TSF) with a pond located at the downstream toe, currently at closure and inactive.
2. A compacted filtered TSF designed over a constructed waste rock dump (WRD).
3. A compacted filtered TSF situated within a valley setting at the design stage.

These configurations represent distinct geometric, operational, and foundation conditions to address solid-to-solid interaction within the context of the GISTM compliance.

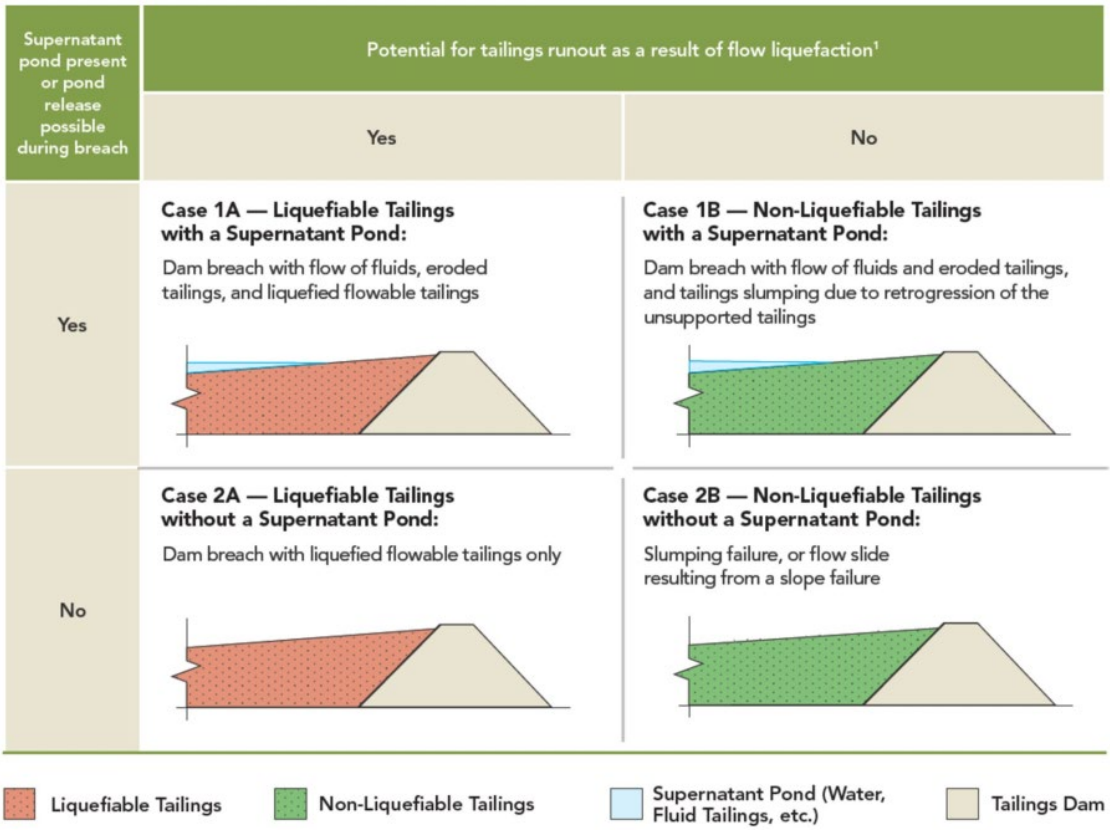

Figure 1 Potential tailings runout scenarios (CDA 2021)

2 Consequence classification

The GISTM provides a full lifecycle framework for safely managing TSFs, integrating risk-informed-decision-making and consequence-based design to prevent catastrophic failures. Developed by the International Council on Mining and Metals, United Nations Environment Programme & Principles for Responsible Investment (ICMM, UNEP & PRI), it emphasises evaluating potential impacts of a hypothetical TSF failure through a consequence classification system that considers population at risk, environmental sensitivity, and socio-economic exposure within the inundation zone.

This classification – ranging from low to extreme – determines the required design standards, governance structures, and independent review processes. Facilities with very high or extreme consequence ratings must meet the most rigorous technical, monitoring, and oversight requirements. Because these ratings depend on accurate runout and inundation modelling, the quality of that analysis directly influences not only the assessment of physical hazards but also the level of emergency planning, community engagement, and operational governance mandated under the standard.

2.1 Release scenarios

In 2021, the CDA updated its *Technical Bulletin on the Application of Dam Safety Guidelines to Mining Dams* incorporating a structured and physics-based approach to tailings dam breach analysis (TDBA) based on the findings of Chen et al. (2014), Martin et al. (2015) and Small et al. (2017). This updated methodology recognises that the character and mobility of released tailings depend primarily on 2 governing factors (Martin et al. 2019):

- presence of supernatant pond or fluid tailings, which increases the potential for hydraulic entrainment
- potential for liquefaction-induced flowability, which may be triggered by various mechanisms, including the breach itself, rapid drawdown, or seismic events.

Based on these factors, CDA defined 4 representative cases that characterise the expected flow behaviour of tailings following a dam breach, as shown in Table 1.

Table 1 Canadian Dam Association (CDA) tailings release scenarios (adapted from CDA 2021)

Release type	Supernatant pond present or pond release possible?	Tailings flow liquefaction potential?	CDA case	Description
Water-dominated	Yes	Yes	Case 1A	Eroded tailings combined with liquefied, flowable tailings producing highly mobile releases
Water-dominated	Yes	No	Case 1B	Eroded tailings with slumping or retrogressive failure of unsupported tailings
Solids-dominated	No	Yes	Case 2A	Liquefied tailings release without significant pond involvement
Solids-dominated	No	No	Case 2B	Slumping failure or flow slide resulting from slope instability and granular collapse

This classification provides a practical decision framework for selecting the appropriate modelling approach during TDBA and for interpreting the results within a consequence-based risk assessment. Beyond defining the expected release mechanism, the CDA classification also establishes the governing parameters required

for numerical modelling of the failure and runout processes. The selected case determines whether the mobilised material should be represented primarily through hydraulic properties or through geomechanical strength parameters.

For water-dominated releases, modelling typically requires characterisation of rheology, water availability, and hydrograph evolution. In contrast, solids-dominated releases are controlled mainly by geotechnical properties such as shear strength, stiffness degradation, failure geometry, and post-failure interaction between soil masses. Consequently, the correct identification of the CDA scenario provides the physical basis for defining the modelling strategy and selecting the governing input parameters for runout analysis.

2.2 Flow regimes and solids concentration

Table 2 relates flow type to solids concentration – by weight and volume – providing an empirical link between material properties and expected runout behaviour.

Table 2 Flow regimes and solids concentration (adapted from O'Brien 1986)

Flow regime	Solids by volume (%)	Solids by weight (%)	Flow characteristics	Applicable Canadian Dam Association cases
Water flood	<20	<41	Fully hydraulic, clear water flow	1A, 1B
Mud flood	35–50	59–69	Mixed flow, wave action, fluid properties	1A, 1B
Mudflow (non-Newtonian)	45–55	69–72	Liquefied tailings at or above liquid limit, fluid-like	1A, 2A
Granular flow; debris flow	55–65	76–83	Slumping of non-liquefied, partly saturated tailings; short runout, solid-to-solid contact	2B

Solids concentration can be expressed either by volume or by weight, both of which are commonly used in the characterisation of tailings flow behaviour. Solids by volume represent the fraction of the total mixture volume occupied by solid particles, which directly controls particle interaction, packing, and mechanical behaviour during mobilisation. Solids by weight represent the mass fraction of solids relative to the total mixture mass and are typically obtained from laboratory measurements or operational data. While both measures describe the same material condition, solids by volume are more directly related to flow mechanics and granular interaction, whereas solids by weight are often more readily available from site monitoring and sampling.

Non-Newtonian flow refers to materials whose apparent viscosity depends on the applied shear stress or strain rate, rather than remaining constant as in Newtonian fluids such as water. Tailings behaving as non-Newtonian mixtures may exhibit yield stress, shear thinning, or plastic behaviour, meaning that flow initiates only after a threshold stress is exceeded. This behaviour is typically associated with partially liquefied or highly saturated tailings and is characteristic of intermediate flow regimes between purely hydraulic transport and fully granular collapse.

For solids-dominated TSFs (Cases 2A and 2B), the expected flow type transitions from non-Newtonian to granular regimes, with minimal water content (w) <25–30%. The breach process in these conditions is better described as a mechanical collapse or flow slide rather than a fluid flood.

2.3 Framework

Once the appropriate case is defined, the consequence classification proceeds through the following key steps:

1. Breach analysis: estimation of breach outflow volume and hydrograph based on flow type and solids content.
2. Runout analysis: simulation of downstream displacement, travel distance, and deposition.
3. Sensitivity analysis: evaluation of key parameter uncertainty.
4. Inundation mapping: delineation of impact zones for consequence classification.

2.4 Modelling tools

GISTM does not prescribe a specific modelling methodology. It requires that the approach be defensible, physics-based, and proportionate to the facility's complexity. In practice, most TDBA applications have been conducted using modelling tools which simulate water-rich flows (i.e. FLO-2D) representative of CDA Cases 1A and 1B. The CDA (CDA 2021) further emphasises that modelling approaches should be selected based on the governing failure behaviour, distinguishing between water-dominated releases (Cases 1A and 1B) and solids-dominated releases (Cases 2A and 2B).

For water-dominated scenarios, breach analyses are commonly performed using hydrodynamic or depth -averaged routing models capable of simulating erosion, entrainment, and fluid transport processes. Commercial tools such as FLO-2D implement depth-averaged hydraulic flow equations with rheological options for non-Newtonian mixtures, while FLOW-3D employs computational fluid dynamics formulations based on the Navier–Stokes equations. MADFLOW similarly applies rheological routing approaches to simulate debris and mudflow-type releases. These modelling approaches are well established for releases involving significant water content and fluidised tailings behaviour (CDA 2021).

However, in solids-dominated scenarios (Cases 2A and 2B), runout is governed primarily by geomechanical instability, progressive collapse, and granular interaction between soil masses, rather than by hydraulic transport. Under these conditions, numerical methods formulated on the conservation of mass and momentum within a continuum geomechanical framework – such as the MPM – provide a more appropriate representation of the failure process. MPM is particularly well suited to modelling geotechnical problems involving large deformations and displacements, as may occur in massive rupture scenarios. This approach enables a realistic simulation of the post-failure behaviour of the system.

3 Material point method

The MPM proposed by Sulsky et al. (1994) is a numerical technique that combines Lagrangian (material) and Eulerian (spatial) descriptions for the solution of problems in continuous media with large deformations. It is based on a hybrid discretisation that represents the domain by means of material points that move through a fixed background mesh (Figure 2).

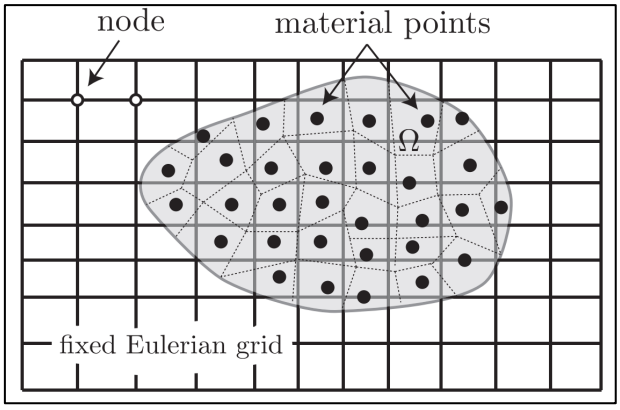

Figure 2 Lagrangian material points superimposed on a Eulerian mesh (Nguyen 2014)

All relevant information in the field (such as mass, velocity, deformations and stresses) is stored at material points. It should be noted that each point does not represent an individual soil particle, but a finite fraction of the domain with its own physical properties and mechanical state.

3.1 Limitations

In the last decade, MPM has been widely adopted for simulating landslides, and a total of 58 cases studies were published between 2015 and May 2024 (Ceccato 2024). First attempts in real cases usually adopted the following simplifications:

- geometry (2D to reduce computational cost)
- constitutive models (non-advanced)
- triggering mechanisms (oversimplified)
- multi-phase behaviour (disregarded).

Recent case studies on TDBA have demonstrated the capability of the MPM to simulate CDA Cases 2A and 2B, confirming the adequacy of the one-phase, single-point formulation for these conditions, including the incorporation of advanced constitutive models to simulate static liquefaction (Cuomo et al. 2019; Robertson et al. 2019; Lino Ramírez 2021; Macedo et al. 2024).

Conversely, multi-phase approaches are more suitable for CDA Cases 1A and 1B (Ceccato et al. 2021; Yerro et al. 2022). Although multi-phase formulations are not yet widely adopted in engineering practice, their application is expected to increase in the coming years. Ongoing advancements in these formulations (i.e. Wang et al. 2024) will enhance their ability to capture the transition from saturated soil-like to water-like flow behaviour (Lino Ramírez et al. 2025; Avilés et al. 2024).

3.2 Material point method formulations

MPM has been implemented in several programming languages. Most versions are currently available as open-source, as shown in Table 3. Some examples of proprietary versions include MPM-PUCRio (Fernández 2020) and MPAC (ITASCA 2025).

Table 3 Open-source codes implementing material point method formulations (Ceccato 2024)

Language	Name of the code
Fortran	Anura3D, COMDYN-MPM3D
C++	CB-Geo, CoSim-MPM (Kratos), Karamelo, MPM-GIMP, NairnMPM, Uintah
MATLAB	AMPLE, fMPMM-solver
Python	MPM-Py

4 Case studies

The analyses were carried out with the Anura3D code (Anura3D 2025), a software used in recent TDBA (Lino Ramírez et al. 2025; Di Carluccio et al. 2024; Alonso 2021), which incorporates MPM implementation based on the MPM-mixed integration interpolation scheme (Zabala & Alonso 2010; Al-Kafaji 2013). Version 17 of the GiD program was used for the generation of the model geometry, the discretisation of the domain and the visualisation of results (International Center for Numerical Methods in Engineering 2024).

4.1 Methodology

The methodology follows a workflow designed to ensure a realistic representation of the geometry, material behaviour, and credible failure modes. The one-phase, single-point formulation was employed in all simulations. Each step is aimed at progressively defining the physical, geotechnical, and numerical

components of the model to achieve stable pre-failure conditions and a reliable simulation of the post-failure response. The main steps of the MPM modelling process are summarised as follows:

1. definition of credible failure modes
2. generation of the geometry and soil layers (2D framework)
3. specification of the constitutive model and geotechnical parameters
4. definition of the number of material points per element
5. definition of boundary conditions (displacement restrictions)
6. generation of the fixed grid (meshing)
7. static phase: stress initialisation to achieve static equilibrium using the design parameters
8. post-failure phase: reduction of the shear strength of selected layers to trigger failure and simulate the subsequent post-failure behaviour.

Table 4 summarises the details of each case study.

Table 4 Details of the case studies

Case study	Configuration	Project stage	Canadian Dam Association case	Description
1	Conventional tailings storage facility (TSF) with a pond located at the toe of the dam	Closure inactive	2A	Cascading effect analysis of the potential failure
2	Compacted filtered TSF placed over a waste rock dump (WRD)	TSF: design WRD: operation	2B	Analysis of the independent potential failure of the TSF, WRD and foundation
3	Compacted filtered TSF placed over a valley	Design	2B	Analysis of a potential failure of the foundation

4.2 Case study 1: conventional tailings storage facility with a pond located at the toe of the dam

A tailings dam failure was simulated to perform a parametric analysis of the runout distance. The runout path of the potential sliding mass included a downstream pond full of water as shown in Figure 3.

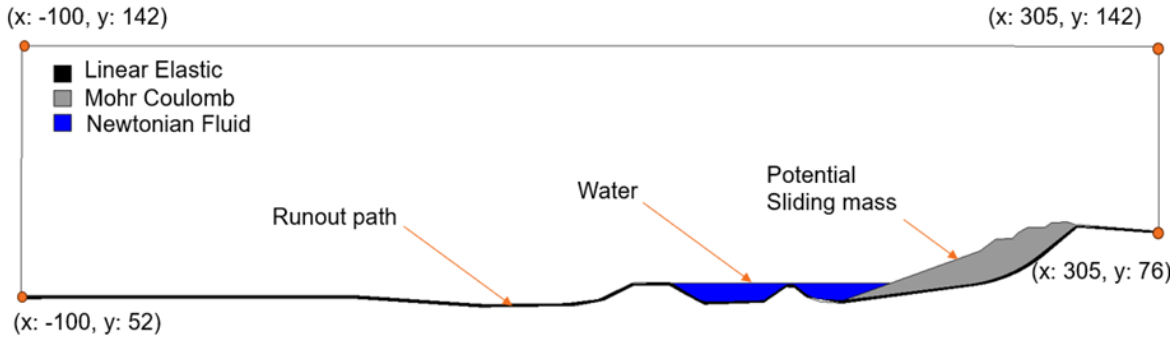

Figure 3 Case study 1: conventional tailings storage facility with a pond located at the toe of the dam

The failure surface was incorporated into the analysis as input data. The sliding mass was adopted as a saturated homogeneous material in undrained condition. A parametric analysis was performed by changing the undrained shear strength, s_u, to estimate the maximum runout distance and its interaction with the water contained between the 2 downstream dykes of the pond.

The models included 3 stages:

1. Stress initialisation using 'gravity loading'.
2. Reduction of the undrained shear strength.
3. Activation of the contact algorithm with enough simulation steps to allow the flow of the sliding mass on the contact surface.

The contact algorithm proposed by Al-Kafaji (2013) was activated, aiming to simulate the undrained shear strength expected along the failure surface and to establish different contact values between the sliding mass and the surface materials present in the runout path (i.e. vegetation, water). The algorithm detects the contact surface and identifies nodes that share information from different materials. If nodal contact forces exceed the failure criteria, relative motion between bodies is allowed (Yerro et al. 2019).

Figure 4 shows the runout path divided into 3 contact surfaces.

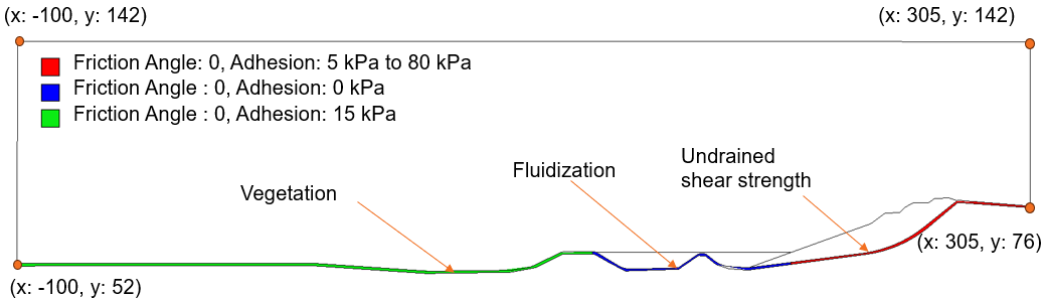

Figure 4 Case study 1: contact surfaces

The constitutive model, Mohr–Coulomb, was selected for the sliding mass, while the contact surfaces along the runout path were considered as linear elastic materials, as summarised in Table 5.

Table 5 Material parameters: case study 1

Property/material	Unit	Sliding mass	Contact surfaces	Water
Constitutive model		Mohr–Coulomb	Linear elastic	Newtonian fluid
Unit weight, γ	kN/m^3	18.5	18.5	10
Poisson's ratio, ν	–	0.45	0.3	–
Elastic modulus, E	MPa	10	50	–
Undrained shear strength, s_u	kPa	5 to 80	–	–
Friction angle, ϕ'	°	0	–	–
Compressibility modulus, K_w	kPa	–	–	2.15×10^4
Dynamic Viscosity, μ_w	kPa.s	–	–	8.90×10^{-7}

Figure 5 shows the fixed grid used in the model, a background mesh of 9,932 elements. The mesh was refined in critical areas and extended to allow the movement of the material points through empty elements.

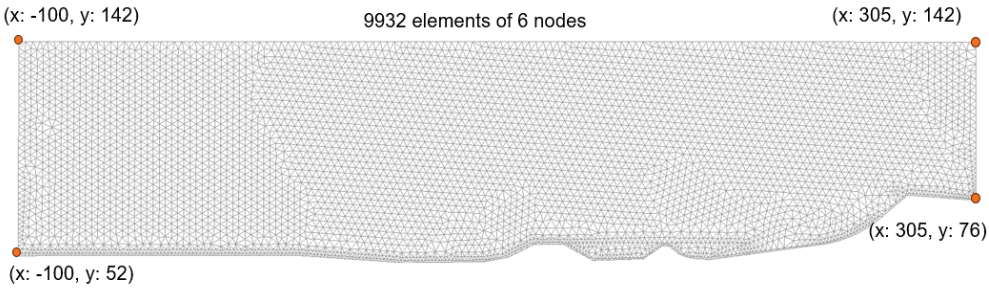

Figure 5 Mesh of the case study 1

Figure 6 shows the summary of the parametric analysis. Varying the undrained shear strength, s_u, of the sliding mass between 5 and 80 kPa resulted in a maximum runout distance of 70 m measured from the slope toe.

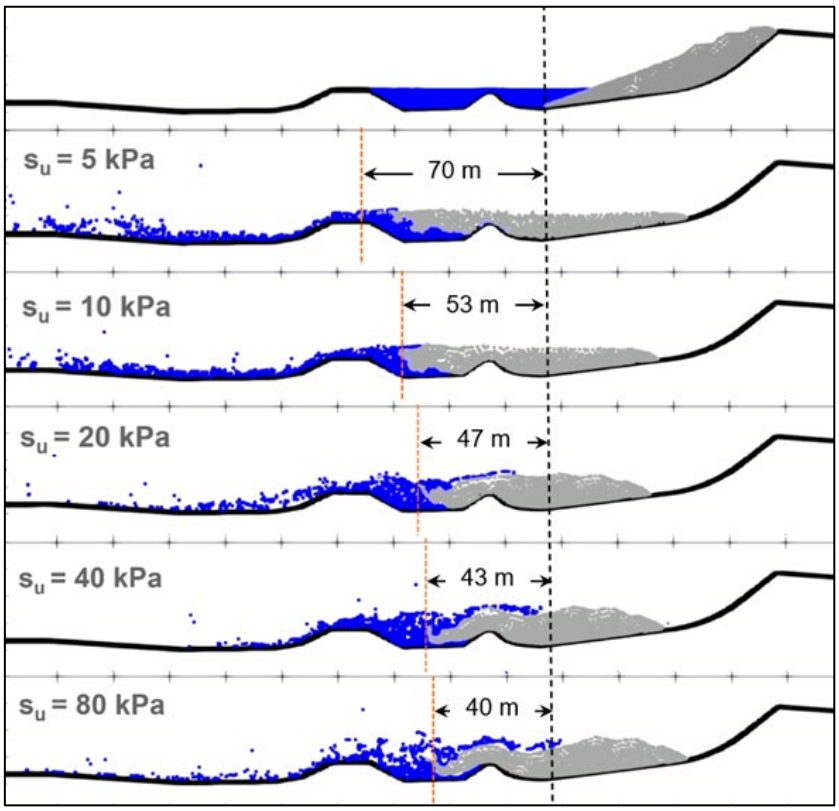

Figure 6 Runout analysis of the case study 1

4.3 Case study 2: compacted filtered tailings storage facility placed over a waste rock dump

The TSF was designed over an existing WRD, which reaches a height of 65 m at its highest point (Figure 7).

Runout distances were estimated for the following credible failure modes:

1. failure of the TSF tailings body
2. global failure of the WRD acting as the foundation of the TSF
3. failure of the natural foundation underlying the WRD.

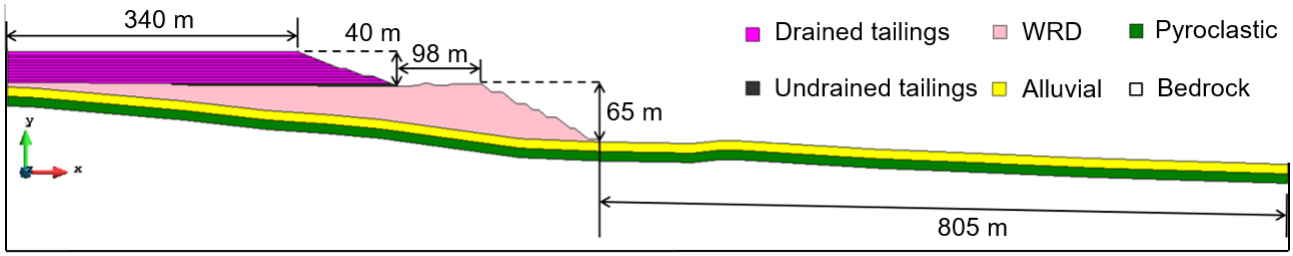

Figure 7 Case study 2: compacted filtered tailings storage facility placed over a waste rock dump (WRD)

The modelling sequence can be summarised in 3 main stages. First, the initial geostatic condition was established (existing WRD and its foundation). Second, the construction of the TSF. Finally, the 3 identified failure modes were simulated.

The Mohr–Coulomb model was used for all materials. The bedrock was considered as a material of infinite extent and strength, idealised as a rigid, non-deformable plane (Table 6).

Table 6 Material parameters: case study 2

Property/material	Unit	Drained tailings	Undrained tailings	Waste rock dump rockfill	Alluvial foundation	Pyroclastic foundation
Unit weight, γ	kN/m^3	16	18	18.20	15	12
Poisson's ratio, ν	–	0.3	0.3	0.3	0.3	0.3
Elastic modulus, E	MPa	10	10	20	30	20
Undrained shear strength, s_u	kPa	–	5	–	–	–
Friction angle, ϕ'	°	31	0	40	39	36
Cohesion, c	°	0	0	0	10	0

A mesh of 4,219 triangular elements was generated (Figure 8). Mesh refinement was applied within the TSF and along the interface with the WRD, where potential failure displacements were expected to occur. The downstream model length was iteratively adjusted to ensure adequate distance between the maximum displacement region and the right boundary.

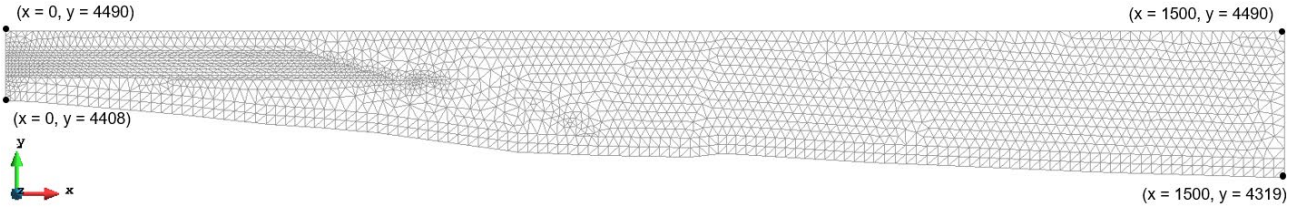

Figure 8 Mesh of the case study 2

To simulate the failure modes, various levels of reduction were applied to the shear strength parameters of the materials involved (Table 7), following the shear strength reduction (SSR) methodology, defined by the expressions:

$$\tan \varphi_r = \tan \varphi / SSR;\ c_r = c / SSR \quad (1)$$

where SSR is the reduction factor applied to the original shear strength parameters ϕ and c to obtain the reduced values ϕ_r and c_r.

An SSR value of 1 represents the design condition without any reduction, i.e. using the original shear strength parameters. Higher SSR values were used to assess the robustness of the design and introduce additional conservatism in estimating potential tailings displacements.

For the TSF, an additional 3 m-thick basal layer with an undrained shear strength of s_u = 5 kPa (Table 7) was incorporated, representing a zone affected by construction deficiencies and modelled as a saturated, undrained material exhibiting residual strength behaviour.

4.3.1 Failure mode 1: tailings storage facility

The failure mode was generated in the numerical model by introducing the low-strength basal layer described in the previous section. This layer was defined with a thickness of 3 m, corresponding to the elevation reached by the TSF after the first year of operation and was modelled with an undrained shear strength of s_u = 5 kPa, representing a saturated material that had lost most of its peak undrained strength.

The modelling sequence for this failure mode began with the completion of the staged construction phase under dry conditions. Once this phase was completed, the basal layer was modified to behave under undrained conditions (by applying s_u = 5 kPa), acting as the triggering mechanism for failure.

Subsequently, progressive reductions in shear strength parameters were applied to the tailing's layers deposited above the initial 3 m and up to the final elevation of the TSF. Since the inclusion of the weak basal layer alone was insufficient to produce significant runout (SSR = 1; Figure 9), the combination with progressive strength reduction in the upper layers enabled the development of more extensive displacements. The results of these scenarios are presented below for SSR values of 2 and 4 (Table 8).

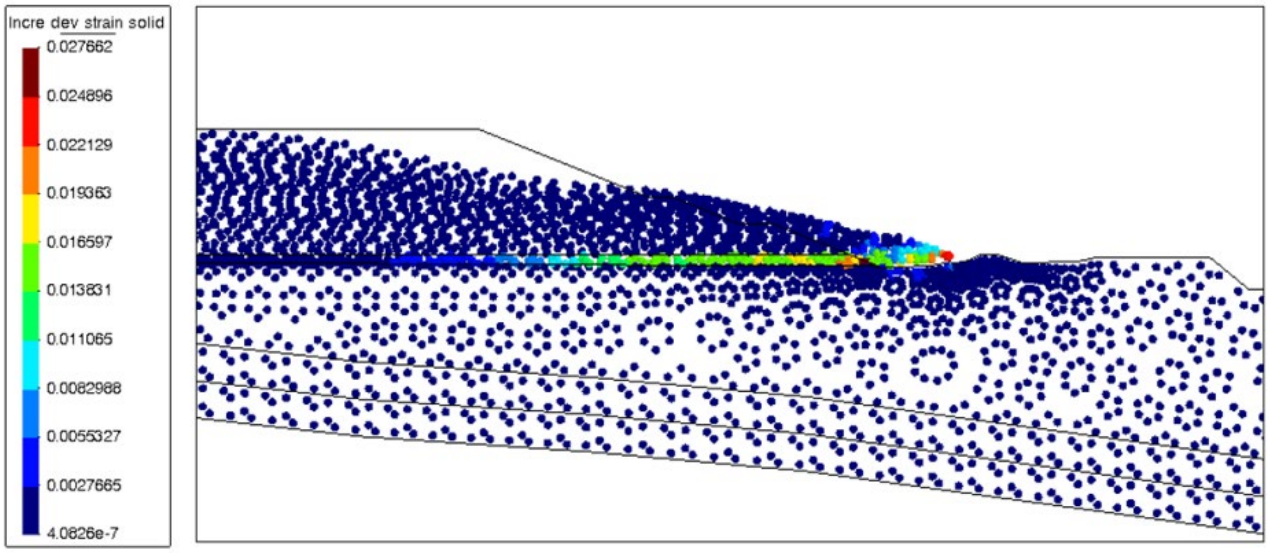

Figure 9 Incremental deviatoric strains: SSR = 1 (case study 2, failure mode 1)

4.3.2 Failure mode 2: waste rock dump

The WRD failure was simulated in the numerical model by reducing its shear strength parameters, considering SSR values of 2 and 4 to represent a hypothetical global instability scenario. This reduction was applied exclusively to the WRD, after completing the staged construction phase under dry conditions. The objective was to evaluate whether such a failure could trigger the displacement of the overlying TSF, resulting in a retrogressive failure mechanism.

4.3.3 Failure mode 3: foundation

A hypothetical foundation failure was simulated by reducing the shear strength parameters of the alluvial layer located at the base of the WRD, with an approximate thickness of 11 m. This reduction was applied exclusively to this layer after completion of the staged construction phase under dry conditions. The objective was to represent a deep-seated translational instability scenario affecting the entire system (TSF and WRD).

4.3.4 Results

Table 7 summarises the runout distances obtained from the MPM simulations, measured from the TSF toe for failure mode 1 (Figure 10) and from the WRD toe for failure modes 2 (Figure 11) and 3 (Figure 12).

Table 7 Results: case study 2

Failure mode	SSR = 1	SSR = 2	SSR = 4	Figure
1	21	64	123	10
2	–	28	250	11
3	–	0.35	15	12

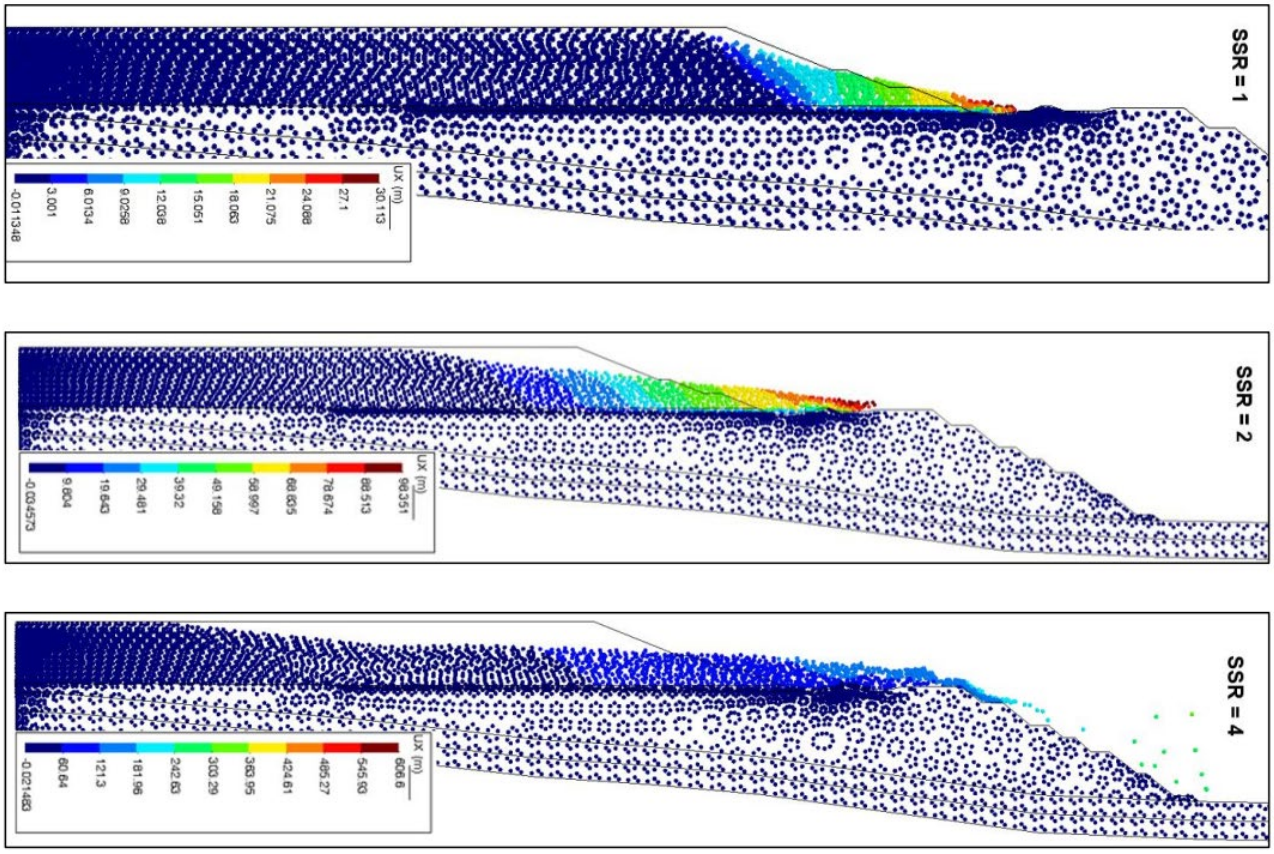

Figure 10 Horizontal displacements, Ux. Failure mode 1

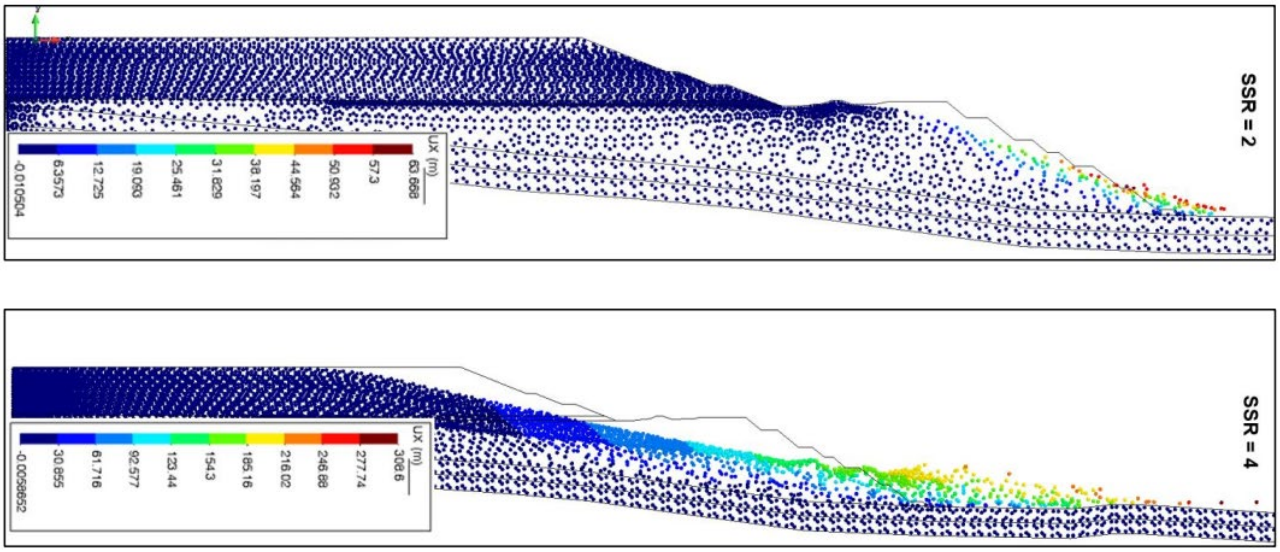

Figure 11 Horizontal displacements, Ux. Failure mode 2

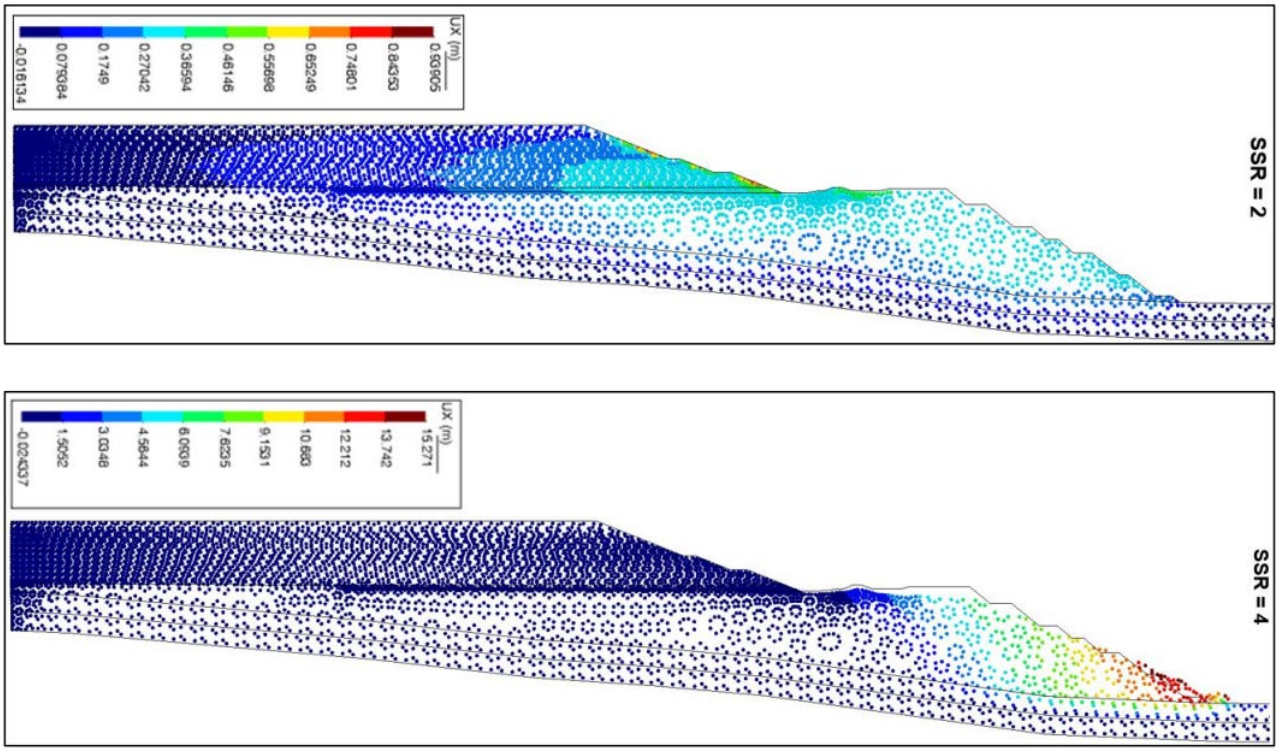

Figure 12 Horizontal displacements, Ux. Failure mode 3

4.4 Case study 3: compacted filtered tailings storage facility placed over a valley

A compacted filtered TSF was designed over a valley characterised by colluvial soils forming the uppermost foundation layer. The TSF reaches a height of 70 m at its highest point (Figure 13).

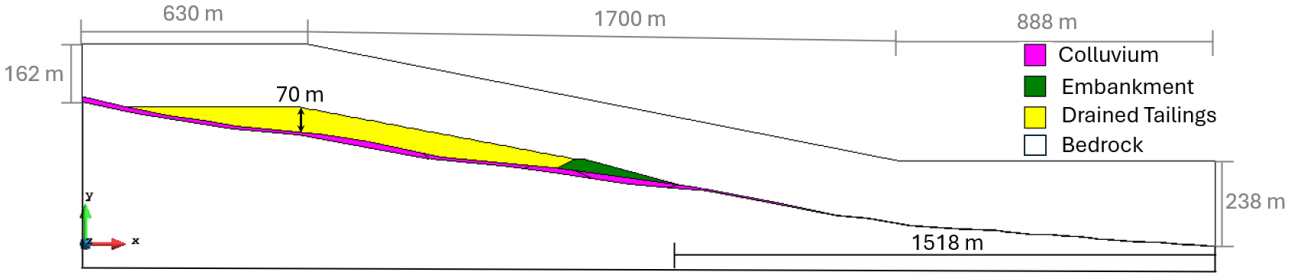

Figure 13 Case study 3: compacted filtered tailings storage facility placed over a valley

To address a maximum runout scenario, the shear strength of the foundation was reduced to trigger the deposit movement. The reduction was applied instantaneously across the entire colluvium layer, including the embankment and tailings footprint. No reduction was applied in the tailings or the embankment materials.

The modelling sequence was carried out in 4 main stages. First, the initial geostatic state of the foundation. Second, the embankment was constructed. Third, the TSF was built to its final configuration, corresponding to the closure stage. Finally, a reduction of the shear strength parameters was applied to the colluvium layer in the foundation to simulate potential failure conditions.

Table 8 summarises the Mohr–Coulomb parameters.

Table 8 Material parameters: case study 3

Property/material	Unit	Colluvium	Reduced colluvium	Embankment	Drained tailings
Unit weight, γ	kN/m^3	19	19	19.7	19.7
Poisson's ratio, ν	–	0.3	0.3	0.3	0.3
Elastic modulus, E	MPa	30	30	10	10
Friction angle, ϕ'	°	35	5	33	33
Cohesion, c'	°	0	0	0	0

A mesh of 2,701 triangular elements was generated (Figure 14). In each element, 12 material points were considered.

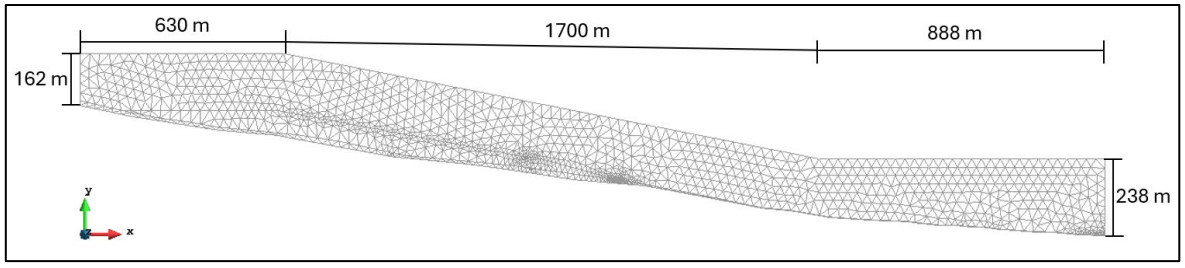

Figure 14 Mesh of the case study 3

The results indicate maximum horizontal displacements of 373 m occurring within a 500 m zone of influence downstream of the embankment slope toe (Figure 15).

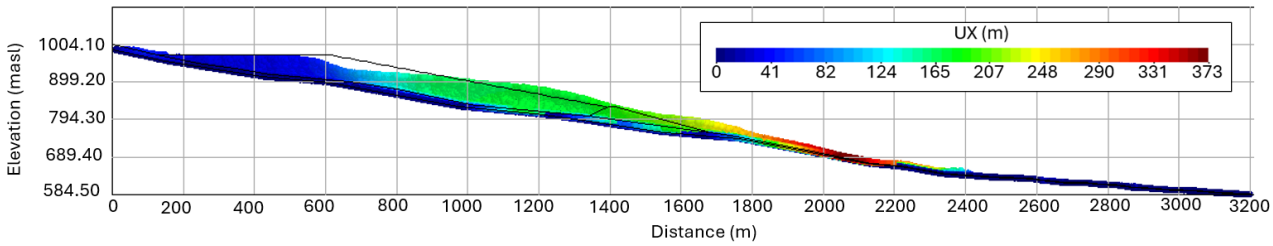

Figure 15 Horizontal displacements, Ux. Case study 3

5 Discussion of results

The numerical simulations performed for the different case studies allowed assessing the influence of the reduction in shear strength parameters on the runout distances.

In Case study 1, the analysis focused on the behaviour of the sliding mass under varying undrained shear strengths of the tailings material, ranging between 5 and 80 kPa. The results indicated a maximum runout distance of approximately 70 m measured from the slope toe.

In all simulated scenarios, the sliding mass ultimately remained confined within the pond's dykes, exhibiting a cascading behaviour that produced different patterns of water release. As the undrained shear strength (s_u) decreased, a larger portion of the tailings mass entered the pond, consequently resulting in greater volumes of water being displaced downstream.

For case study 2, 3 potential failure modes were examined:

- Failure mode 1 (TSF): for SSR = 1, the mobilised tailings mass halted before reaching the containment embankment, with a runout distance of approximately 21 m. When SSR = 2, the displaced tailings overtopped the containment embankment but stopped before reaching the WRD crest (runout ~64 m). At SSR = 4, the mobilised material surpassed the WRD crest, resulting in an estimated runout distance of 123 m.
- Failure mode 2 (WRD): with SSR = 2, the failure induced displacements along the WRD benches without affecting the overlying TSF (runout ~28 m). At SSR = 4, the instability of the WRD involved a significant portion of the TSF, producing a runout distance of about 250 m.
- Failure mode 3 (foundation): for SSR = 2, displacements throughout the system were minimal (runout ~0.35 m). When SSR = 4, limited displacements were observed near the toe and crest of the WRD, but no global failure of the system or impact on the TSF was observed (runout ~15 m).

Finally, in case study 3, where the foundation beneath the TSF was weakened, the model predicted maximum horizontal displacements of 373 m, with deformation extending within a 500 m influence zone downstream of the embankment slope.

6 Conclusions

The results of this study demonstrate that the MPM provides a robust framework for runout analysis of CDA Cases 2A and 2B, enabling more comprehensive and physically consistent evaluations in accordance with the GISTM.

As the runout extent delineates the inundation zone, it directly governs the population at risk and, consequently, the consequence classification under the GISTM framework. If hydraulic-based approaches continue to be applied to CDA Cases 2A and 2B, the resulting inundation areas may be artificially enlarged, leading to inflated consequence classifications. This has important implications, as facilities categorised as extreme or very high consequence must undergo independent technical reviews and comply with the most stringent design and monitoring standards under the GISTM framework.

Despite current limitations, the use of the MPM in this study represents a technically sound and consistent approach, aligned with the material characteristics, the expected failure mechanism, and the objectives of the analysis. In particular, the constraints do not significantly affect its applicability to the presented cases. Therefore, the method adequately captures the behaviour of the compacted filtered stacks or dewatered deposits following failure.

Acknowledgement

The authors express their gratitude to Dr Luis A Avilés Murcia for his insightful discussions on the application of the MPM, and to the Anura3D Research Community for promoting open knowledge and collaboration.

References

Al-Kafaji, I 2013, *Formulation of a Dynamic Material Point Method (MPM) for Geomechanical Problems*, PhD thesis, University of Stuttgart, Stuttgart.

Alonso, E 2021, 'Triggering and motion of landslides', *Géotechnique*, vol. 71, no. 1, pp. 3–59.

Anura3D 2025, 'Open-source version to model large deformation and soil-water-structure interaction with the MPM', *Github,* https://github.com/Anura3D/Anura3D_OpenSource

Avilés, L, Di Carluccio, G & Pinyol, N 2024, 'Layered construction process with the material point method', *Computers and Geotechnics*, vol. 171, https://doi.org/10.1016/j.compgeo.2024.106401

BioBioChile 2024, *FOTOS | Falla en muro de contención provocó emergencia por relaves mineros en región de Valparaíso,* https://www.biobiochile.cl/noticias/nacional/region-de-valparaiso/2024/06/14/fotos-falla-en-muro-de-contencion-provoco-emergencia-por-relaves-mineros-en-region-de-valparaiso.shtml

Canadian Dam Association 2021, *Technical Bulletin: Application of Dam Safety Guidelines to Mining Dams*, Ottawa.

Ceccato, F, Yerro, A & Di Carluccio, G 2024, 'Simulating landslides with the material point method: best practices, potentialities, and challenges', *Engineering Geology*, vol. 338, https://doi.org/10.1016/j.enggeo.2024.107614

Ceccato, F, Yerro, A, Girardi, V & Simonini, P 2021, 'Two-phase dynamic MPM formulation for unsaturated soil', *Computers and Geotechnics*, vol. 129.

Chen, Z, Martin, T, McRoberts, E & Davies, M 2014, 'A review of methods for predicting the runout of tailings dam failures', *Tailings and Mine Waste' 14: Proceedings of the 18th International Conference on Tailings and Mine Waste*, The University of British Columbia, Vancouver

International Center for Numerical Methods in Engineering 2024, *GiD: The Personal Pre and Post Processor*, Barcelona, https://www.gidsimulation.com/gid-for-science/downloads/

Cuomo, S, Ghasemi, P, Martinelli, M & Calvello, M 2019, Simulation of liquefaction and retrogressive slope failure in loose coarse-grained material', *International Journal of Geomechanics*, vol. 19, no. 10.

Di Carluccio, G, Pinyol, N, Alonso, E & Hürlimann, M 2024, 'Liquefaction-induced flow-like landslides: the case of Valarties (Spain)', *Géotechnique*, vol. 74, no. 4, pp. 307–324.

Fernández, F 2020, *Modelagem Numérica de Problemas Geotécnicos de Grandes Deformações Mediante o Método do Ponto Material*, PhD thesis, Pontifícia Universidade Católica, Rio de Janeiro.

International Council on Mining and Metals, United Nations Environment Programme & Principles for Responsible Investment 2020, *Global Industry Standard on Tailings Management*, London.

ITASCA 2025, *Material Point Analysis Code*, Minneapolis.

Jaguar Mining Inc. 2024, *Operational Update Following Slope Failure at Turmalina Mine*, Toronto.

Lino Ramírez, E 2021, *Modelling of Flow Liquefaction and Large Deformations in Tailings Dams Using Material Point Method*, Masters thesis, The University of British Columbia, Vancouver.

Lino Ramírez, E, Ledesma, O & Lizcano, A 2025, 'Runout analysis using the material point method (MPM) for CDA Cases 2a and 2b', *CDA 2025 Annual Conference*, Canadian Dam Association, Markham.

Morgenstern, NR, Vick, SG, Viotti, CB & Watts, BD 2016, *Fundão Tailings Dam Review Panel: Report on the Immediate Causes of the Failure of the Fundão Dam*, Prepared for Cleary Gottlieb Steen & Hamilton LLP.

Macedo, J, Yerro, A, Cornejo, R & Pierce, I 2024, 'Cadia TSF failure assessment considering triggering and post triggering mechanisms', *Journal of Geotechnical and Geoenvironmental Engineering*, vol. 150, no. 4.

Martin, T, Davies, M, Chen, Z & McRoberts, E 2015, 'Towards a risk-informed tailings dam breach analysis', *Proceedings of Tailings and Mine Waste 2015*, University of Alberta Geotechnical Centre, Vancouver, pp. 255–266.

Martin, T, Small, J, Jeeravipoolvarn, S, McRoberts, E, Chen, Z & Davies, M 2019, 'Characterizing the behaviour of released tailings for dam breach consequence assessment', *Proceedings of Tailings and Mine Waste 2019*, University of Alberta Geotechnical Centre, Vancouver, pp. 193–206.

Nguyen, V 2014, *Material Point Method: Basics and Applications*, Institute of Advanced Mechanics and Materials, Cardiff University, Cardiff.

O'Brien, J 1986, 'Physical and mathematical modelling of debris flow', *Proceedings of the Specialty Conference on Delineation of Landslide, Flash Flood, and Debris Flow Hazards in Utah*, Utah State University, Logan.

Petley, D 2024, *The Turmalina Mine Waste Landslide in Brazil: The Landslide Blog*, American Geophysical Union, Washington.

Reporte Minero 2025, *Multa a Minera Las Cenizas por contaminación del Río Ligua tras colapso de relaves*, https://www.reporteminero.cl/noticia/noticias/2025/06/multa-minera-las-cenizas-por-contaminacion-del-rio-ligua

Robertson, P, de Melo, L, Williams, D & Wilson, G 2019, *Report of the Expert Panel on the Technical Causes of the Failure of Feijão Dam I*, report prepared for Vale S.A.

Small, J, Martin, T, Jeeravipoolvarn, S, McRoberts, E, Chen, Z & Davies, M 2017, Tailings dam breach analysis: a state-of-practice review, *Proceedings of the Canadian Dam Association Annual Conference 2017*, Canadian Dam Association, Markham, pp. 1–15.

Sulsky, D, Chen, Z & Schreyer, H 1994, 'A particle method for history-dependent materials', *Computer Methods in Applied Mechanics and Engineering*, vol. 118, no. 1–2, pp. 179–196.

Wang, Y & Wu, W 2024, 'Numerical model for solid-like and fluid-like behavior of granular flows', *Acta Geotechnica*, vol. 19, pp. 6483–6494.

Yerro, A, Girardi, V, Martinelli, M & Ceccato, F 2022, 'Modelling unsaturated soils with the material point method, a discussion of the state-of-the-art', *Geomechanics for Energy and the Environment*, vol. 32.

Yerro, A, Soga, K & Bray, J 2019, 'Runout evaluation of Oso landslide with the material point method', *Canadian Geotechnical Journal*, vol. 56, no. 9, pp. 1304–1317.

Zabala, F & Alonso, E 2010, *Modelación de problemas geotécnicos hidromecánicos utilizando el Método del Punto Material*, PhD thesis, Universidad Politécnica de Catalunya, Barcelona.